Synchronization of multiple spark-gap switches by a transmission line transformer

Synchronization of multiple spark-gap switches by a transmission line transformer

Z. Liu,[a)] K. Yan, A. J. M. Pemen, G. J. J. Winands, and E. J. M. Van Heesch
EPS group, Faculty of Electrical Engineering, Technology University of Eindhoven, 5600 MB Eindhoven, The Netherlands

(Received 26 August 2005; accepted 3 October 2005; published online 28 November 2005)

A transmission line transformer (TLT)-based multiple-switch circuit topology was recently proposed for pulsed-power generation. By means of a TLT, multiple spark-gap switches can be synchronized in a short time (ns). It is attractive to be used to design a long-lifetime repetitive large pulsed-power source (100 kW, 1 kHz) for various kinds of applications, such as corona plasma-induced gas cleaning. To gain insight into the synchronization principle and switching behavior of the individual switch, an equivalent circuit model was developed and an experimental setup with two spark-gap switches and a two-stage TLT has been constructed. We observed that in terms of switching currents, the two switches can be synchronized within 2–3 ns. The equivalent circuit model approximately fits the experimental results. © *2005 American Institute of Physics.*
[DOI: 10.1063/1.2132269]

I. INTRODUCTION

For generation of high pulsed power, multiple-switch-based circuit topologies are often used to produce high-voltage or large-current pulse and/or their combination. When the multiple switches are used in series, e.g., the Marx generator,[1,2] large pulsed-power generation is realized by producing a higher-voltage pulse. On the other hand, when the multiple switches are used in parallel, for instance, in a capacitor bank,[3] large pulsed-power generation is realized by producing a large-current pulse. Obviously, the most critical issue for the utilization of multiple switches is how to synchronize them within a short period. In general, specially designed synchronization trigger circuits are needed.

A multiple-switch circuit topology for repetitive large pulsed-power generation was proposed in 2001.[4] The circuit is based on a transmission line transformer[5,6] (TLT) and multiple switches which are used in parallel. This topology was successfully verified in a small-scale model with three spark-gap switches.[7] As a result, we started to investigate this circuit topology in detail in order to develop a long-lifetime repetitive (1 kHz), large peak (1 GW), and average power (100 kW) pulsed-power source for corona plasma applications.[8] In order to evaluate the synchronization principle and switching behavior of the individual switches, an experimental setup with two spark-gap switches and a two-stage TLT has been constructed and its equivalent circuit model was derived. Details are presented in this article.

II. PRINCIPLE OF MULTIPLE-SWITCH PULSED-POWER CIRCUIT

Figure 1 shows the schematic diagram of a multiple-switch circuit with two spark-gap switches S_1 and S_2 and a two-stage TLT. Magnetic cores are placed around the transmission lines to increase the impedance Z_s, which is defined as the wave impedance between the two adjacent stages of the TLT as seen from the input side. At the input side of the TLT, the two identical capacitors C_1 and C_2 are charged in parallel up to V_0. They are connected to the transmission lines via the two switches. Whenever one of the two switches is closed, there will be a voltage pulse traveling between the two transmission lines.[2] As a consequence, an overvoltage

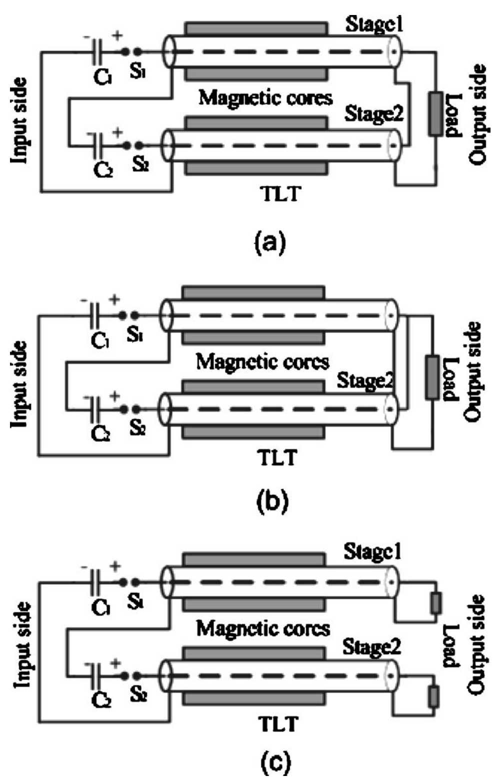

FIG. 1. Schematic diagrams of the circuit topologies with two switches and a two-stage TLT. (a) TLT is used in series at the output side. (b) TLT is used in parallel at the output side. (c) TLT is used for two independent loads.

[a)]Electronic mail: z.liu@tue.nl

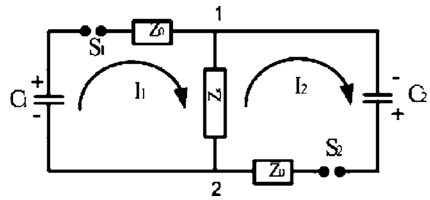

FIG. 2. Equivalent circuit for the input side of the TLT. I_1 and I_2 are the switching currents in S_1 and S_2, respectively.

will appear over the other switch, forcing it to close as well. At the output side, the transmission lines can be connected in various ways: (i) in series to generate a high-voltage pulse; (ii) in parallel to produce a large-current pulse; or (iii) can be used to drive two independent loads. In Fig. 1(a), the TLT is connected in series at the output side. The output impedance, voltage, and current are $2Z_0$, $2V_0$, and I_0, respectively, where I_0 is the switching current and Z_0 is the impedance of the each transmission line. In Fig. 1(b), the TLT is connected in parallel at the output side, thus the output impedance of the TLT, the voltage, and the current are $Z_0/2$, V_0, and $2I_0$, respectively. In Fig. 1(c), the TLT is connected to two independent loads to drive them simultaneously. The three circuits shown in Fig. 1 will give an identical output power, but at different voltage and current outputs.

If we suppose that the TLT is ideally matched at the output side and the transit time for a pulse propagating along the outsides of the transmission lines is much longer than the pulse duration, a simplified equivalent circuit for the input side of the TLT can be derived, in Fig. 2.

Because the impedance Z_s is designed to be much larger than the characteristic impedance Z_0, a voltage V_{12} is generated over the impedance Z_s whenever one switch is closed and the other one is still open. Now the capacitors C_1 or C_2 will discharge very slowly due to the large Z_s. The voltage V_{12} over Z_s is equal to $[Z_s(Z_0+Z_s)]V_0=V_{12}\approx V_0$, where V_0 is the charging voltage on the capacitors. Moreover, because the stray capacitance of the spark-gap switch S_1 or S_2 is much smaller than the capacitance of C_1 or C_2, the voltage across the unclosed switch rises from V_0 to $V_0+V_{12}\approx 2V_0$. This generated overvoltage will remain until the second switch is closed.

When all the switches are closed, one can derive the following equations for the equivalent circuit of Fig. 2:

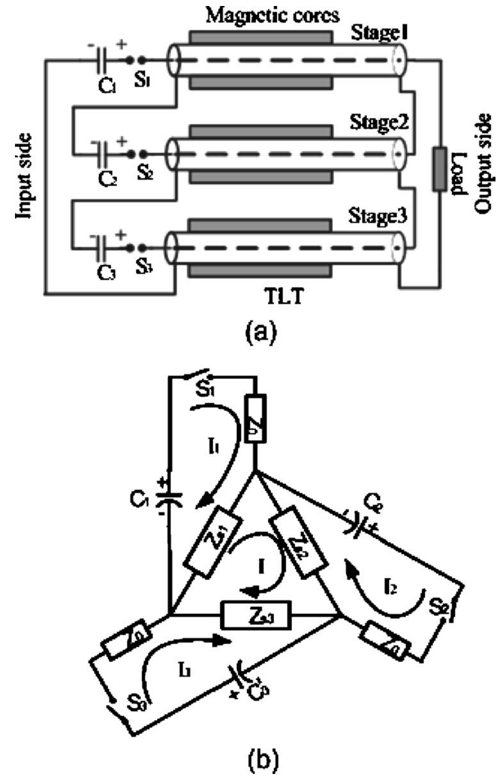

FIG. 3. Circuit topology with three switches and a three-stage TLT and its equivalent circuit referred to the input side. (a) Three-switch circuit topology. (b) Equivalent circuit referred to the input side.

$$I_1(t)(Z_0+Z_s)-I_2(t)Z_s=V_0-\frac{1}{C_0}\int_0^t I_1(\tau)d\tau, \tag{1}$$

$$I_2(t)(Z_0+Z_s)-I_1(t)Z_s=V_0-\frac{1}{C_0}\int_0^t I_2(\tau)d\tau, \tag{2}$$

where $I_1(t)$ and $I_2(t)$ are the currents flowing in switches S_1 and S_2, respectively, and C_0 is the value of the capacitors C_1 and C_2. Solving these two equations, one obtains the following expression for $I_1(t)$ and $I_2(t)$:

$$I_1(t)=I_2(t)=\frac{V_0}{Z_0}\exp\left(\frac{-t}{Z_0C_0}\right). \tag{3}$$

After both switches are closed, the currents $I_1(t)$ and $I_2(t)$ are identical and the voltage V_{12} across the secondary mode impedance Z_s drops to zero. The two switches equally

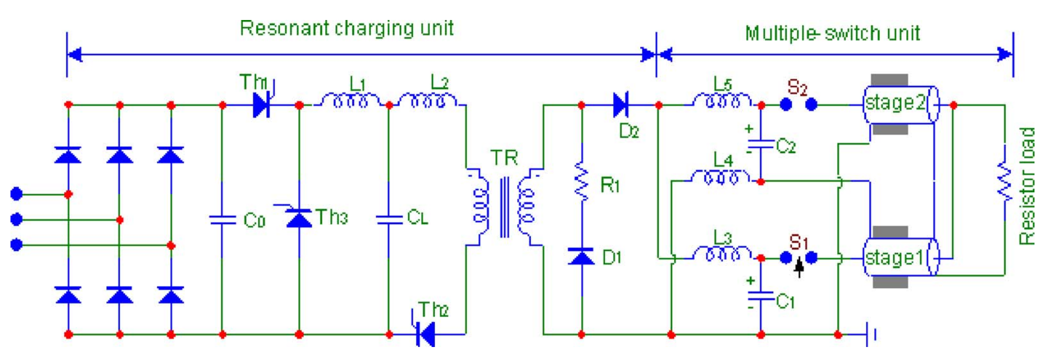

FIG. 4. Schematic diagram of the main circuit of the experimental setup.

share the total current (I_1+I_2) and they are used in parallel equivalently. For a real circuit, though this simplified equivalent circuit cannot be used to accurately derive the switching current due to limited secondary impedance and the length of the TLT, the model presents the fundamental principle of the circuit.

In principle, the above-described hypothesis can be used for any n-stage TLT. As an example, Fig. 3 gives the schematic diagram of a three-switch circuit topology and its equivalent circuit at the input side. In Fig. 3(a), three identical capacitors are connected to the transmission lines via three switches, and the transmission lines are connected in series at the output side. Figure 3(b) gives the equivalent circuit for the input side, where Z_{s1}, Z_{s2}, and Z_{s3} are the impedances between lines 1 and 3, lines 1 and 2, and lines 2 and 3, respectively. Similar to the case with two switches, one can analyze the circuit and derive the circuit equations. More examples of such circuit topologies were reported elsewhere.[7] In addition, the capacitors used in the presented circuits can be replaced by transmission lines to obtain square pulses. Other kinds of switches, such as solid-state switches and magnetic compression switches, can be used to replace the spark-gap switches.

III. EXPERIMENTAL SETUP

Figure 4 shows the circuit diagram of the present experimental setup. It includes a resonant charging unit and a two-switch pulsed-power circuit unit.

The resonant charging source was previously developed in our group.[4] It accomplishes one charging period through three steps: first of all, the thyristor Th_1 closes to resonantly charge the capacitor C_L via the inductor L_1; second, the thyristor Th_2 closes to resonantly charge the high-voltage capacitors C_1 and C_2 via pulse transformer TR; finally, before the next pulse, the thyristor Th_3 closes to reverse the polarity of voltage on C_L in order to keep the system within a safe region when a mismatch occurs. Details were reported earlier.[4] The charging unit can charge the high-voltage capacitors C_1 and C_2 up to 30 kV at a repetition rate of up to 1000 pulses per second (pps).

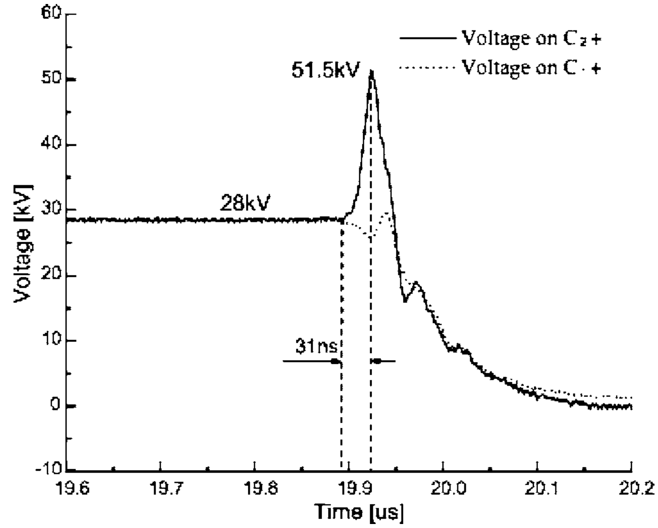

FIG. 5. Typical wave form of the voltage on C_{1+} and C_{2+}, respectively, before, during, and after the synchronization of S_1 and S_2; C_{1+} and C_{2+} refer to the positive end of C_1 and C_2.

The multiple-switch unit consists of three 150 μH air-core inductors L_3, L_4, and L_5, two 1.3 nF high-voltage (dc 40 kV) capacitors C_1 and C_2, two air-flushed spark-gap switches S_1 and S_2, a two-stage TLT, and a resistive load. The inductors show high impedance during the switch synchronization. As for the two switches, S_1 is an *LCR* triggered spark-gap switch[9] and S_2 is a self-breakdown spark-gap switch. After the high-voltage capacitors are charged, the switch S_1 is triggered and closes first, then switch S_2 is fired due to the overvoltage. The TLT is made from 1.5 m coaxial cable RG217 (50 Ω), and the distance between the outer conductors of two cables is about 10 cm. The transmission lines are put in parallel and are matched by a 25 Ω resistor load at the output side. Magnetic cores (MP4510) are placed

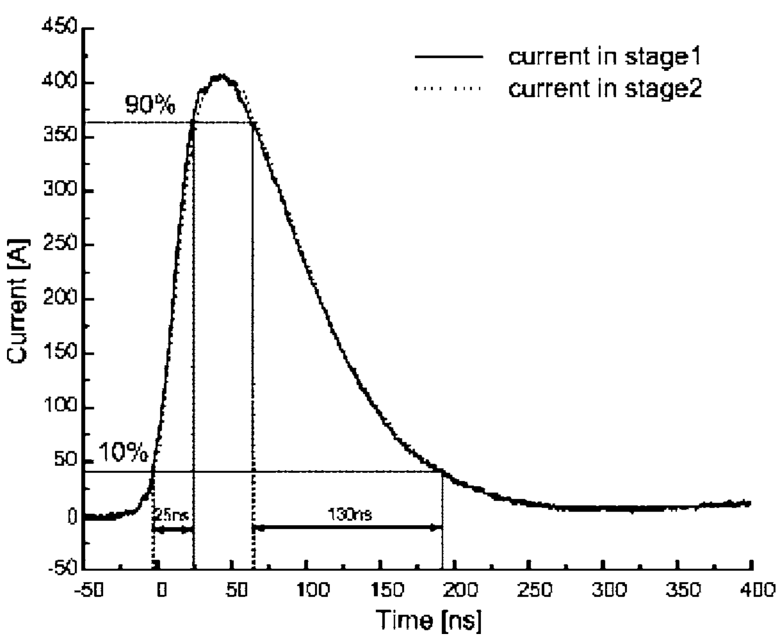

FIG. 6. Typical wave forms of the currents in stages 1 and 2 when C_1 and C_2 are 1.3 nF.

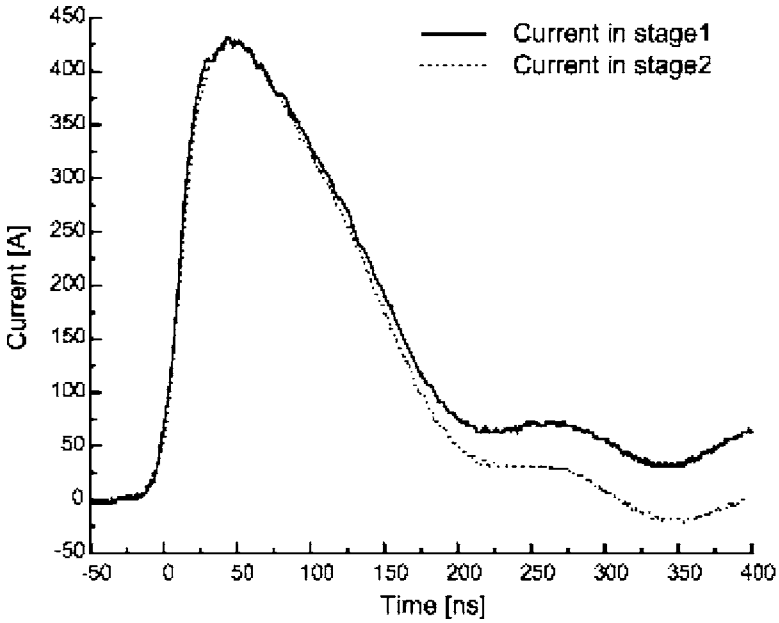

FIG. 7. Typical wave forms of currents in stages 1 and 2 when C_1 and C_2 are 2.6 and 1.3 nF, respectively.

around the cables to increase the impedance Z_s. The length covered by the magnetic cores on each cable is 1 m.

With the present setup, the pulse repetition rate was limited to 20 pps. According to our experience on gas-flushed spark-gap switches, the setup can be used for up to 1000 pps when the two switches are replaced by high-pressure gas-flushed spark-gap switches.

IV. EXPERIMENTAL RESULTS AND DISCUSSION

Figure 5 gives typical voltage wave forms on the capacitors C_1 and C_2. They clearly show the voltage transient before, during, and after the synchronization of S_1 and S_2. The measurements were performed with a Northstar high-voltage probe PVM-1 (ratio of 1000:1, bandwidth of 80 MHz). The capacitors C_1 and C_2 are charged to 28 kV. The triggered spark-gap switch S_1 is closed firstly. Then the voltage on the positive end of C_2 rises to 51.5 kV (equal to 92% of two times 28 kV), which forces the self-breakdown spark-gap switch S_2 to close. The 31 ns rise time (from 28 to 51.5 kV) of the overvoltage pulse means that switch S_2 closes 31 ns after the switch S_1 has closed.

Figure 6 gives typical current wave forms in both stages of the TLT. The measurements were performed with Pearson current transformers (Model 6600) placed around the leads to the negative end of the capacitors. The two current pulses are almost identical, and their time delay is around 2–3 ns. Thus, we can conclude that the output currents in both stages are synchronous within 2–3 ns. The rise time of the current pulse is about 25 ns. The fall time of pulse, e.g., the time required for the current to drop from 90% to 10% of the peak value, is about 130 ns, which is approximately equal to 2τ (τ is defined as time constant and equal to Z_0C_0). An ideal damped exponential curve has a 90%–10% decay time of 2.2τ. One can conclude that Eq. (3) obtained from the equivalent circuit model approximately fits the observed results. Furthermore, referring to both voltage and current wave forms shown in Figs. 5 and 6, we can conclude that even though the two spark-gap switches close within a relatively long period (31 ns), the capacitors, however, can only be discharged simultaneously (when all switches have closed). It is this property that makes the circuit unique in comparison with other type of multiple-switch pulsed-power circuits.

In order to illustrate the circuit's sensitivity to the value of the main components, Fig. 7 plots typical current wave forms in the case that C_1 is 2.6 nF and C_2 is 1.3 nF. As observed with two identical capacitors, there is no problem at all for their synchronization. But in this case, an oscillation at the end of the pulse can be observed due to mismatched capacitors. The pulse duration is mainly determined by the small capacitor, and the oscillation is mainly affected by the difference in capacitance. For highly efficient pulsed-power generation, identical capacitors are needed.

ACKNOWLEDGMENT

The authors thank the Dutch IOP EMVT Program for supporting this work.

[1] X. Wang, Z. Zhang, C. Luo, and M. Han, the 12th IEEE Pulsed Power Conference, 27–30 June 1999, Vol. 2, pp. 815–817.
[2] M. G. Grothaus, S. L. Moran, and L. W. Hardesty, Power Modulator Symposium, 23–25 June 1992, p. 119.
[3] S. T. Pai and Q. Zhang, *Introduction to High Power Pulse Technology* (World Scientific, London, 1995).
[4] K. Yan, Ph. D thesis, Technische Universiteit Eindhoven, 2001; http://alexandria.tue.nl/extra2/200142096.pdf
[5] P. W. Smith, *Transient Electronics: Pulsed Circuit Technology* (Wiley, Chichester, 2002).
[6] J. O. Rossi and P. W. Smith, IEEE Pulsed Power Conference, March 1997, pp. 1–3.
[7] K. Yan, H. W. M. Smulders, P. A. A. F. Wouters, S. Kapora, S. A. Nair, E. J. M. van Heesch, P. C. T. van der Laan, and A. J. M. Pemen, J. Electrost. **58**, 221 (2003).
[8] K. Yan, E. J. M. van Heesch, P. A. A. F. Wouters, A. J. M. Pemen, and S. A. Nair, 25th International Power Modulator Symposium and 2002 High-Voltage Workshop, Conference Record of the Twenty-Fifth International, 30 June–3 July 2002, pp. 420–423.
[9] K. Yan, E. J. M. van Heesch, S. A. Nair, and A. J. M. Pemen, J. Electrost. **57**, 29 (2003).